HETEROCYCLES, Vol. 99, No. 2, 2019, pp. 1251 - 1275. © 2019 The Japan Institute of Heterocyclic Chemistry
Received, 29th October, 2018, Accepted, 3rd December, 2018, Published online, 27th February, 2019
DOI: 10.3987/COM-18-S(F)99

DIASTEREO–/ENANTIOSELECTIVE DIELS–ALDER SYNTHESIS OF 14β-HYDROXYSTEROID SCAFFOLDS: A COMBINED EXPERIMENTAL AND DFT STUDY

Clovis Peter,[†] Philippe Geoffroy,[†] Takatsugu Murata,[§] Takayuki Tonoi,[§] Isamu Shiina,[§]* and Michel Miesch,[†]*

[†]Institute of Chemistry–UMR 7177, University of Strasbourg, 4 rue Blaise Pascal CS 90032, 67081 Strasbourg Cedex-France. E-mail: m.miesch@unistra.fr
[§]Department of Applied Chemistry, Faculty of Science, Tokyo University of Science, 1-3 Kagurazaka, Shinjuku-ku, Tokyo 162-8601, Japan. E-mail: shiina@rs.kagu.tus.ac.jp

The authors dedicate this paper to Professor Dr. Tohru Fukuyama on the celebration of his 70th birthday.

Abstract – Natural, non-natural and *ent*-14β-hydroxyandrostane derivatives closely related to the cardenolide and bufadienolide skeletons were readily available through highly diastereo-/enantioselective Diels–Alder reactions calling for high pressure or Lewis acid activation. Moreover, in the presence of (*R*)- or (*S*)-carvone as chiral dienophile, the Diels–Alder reaction took place under chemodivergent parallel kinetic resolution control. Based on experimental and DFT studies, reasonable mechanism insights were postulated to explain the concave/convex and *endo*/*exo* selectivities observed for the formation of the different Diels–Alder and Diels–Alder–Michael adducts.

INTRODUCTION

The 14β-hydroxyandrostane core represents an important framework found in numerous bioactive steroids. For example, 14β-hydroxysteroids bearing a $\Delta^{5,6}$-double bond were extracted from plants belonging to the *Asclepiadaceae* family and showed appetite suppressant properties (hoodigoside **1**).[1] On the other hand, cardenolides (ouabain **2**, digitoxin **3**) and bufadienolides (bufalin **4**) known as cardiotonic steroids, show potent cardiotonic activity.[2] It has also been suggested that this class of compounds may be useful for cancer therapies.[3] Cardenolides and bufadienolides share a characteristic steroid-like-

framework that is distinct from conventional androstane/pregnane-type steroids in that they have *cis* A/B and C/D ring junctions (**Figure 1**).

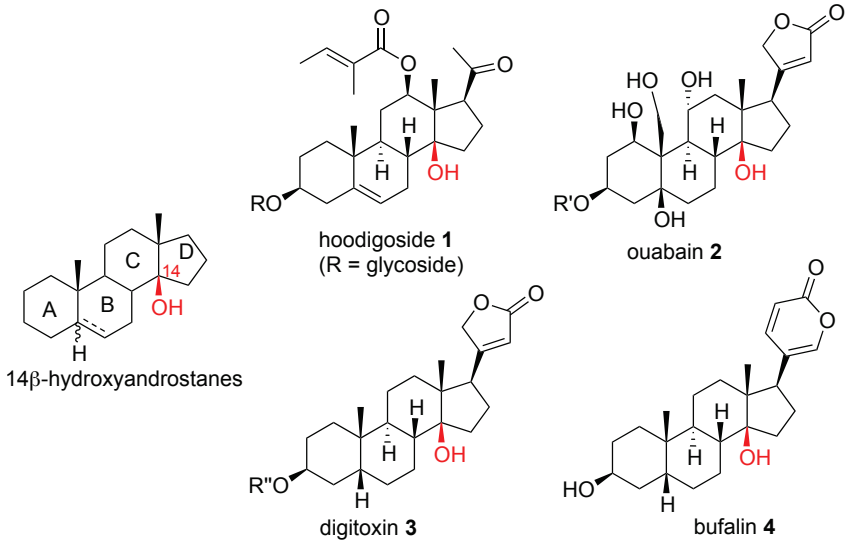

Figure 1. Natural 14β-hydroxysteroids

The access to the 14β-hydroxyandrostane core can be achieved using different methodologies. Oxidation of the 14,15-double bond,[4] polyanionic cyclization,[5] aldol reaction,[6] radical cyclization,[7] inverse demand Diels–Alder[8] and organocatalyzed reactions[9] represent the main routes for the construction of the 14β-hydroxyandrostane framework. It should also be noticed that a renewed interest for the total synthesis of 14β-hydroxysteroids took recently place because the synthesis of the latter is highly challenging and analogs could be evaluated for their biological properties.[4g,4h,5h,6c-e]

Given that natural 14β-hydroxysteroids (existing only as one enantiomeric form) have an important array of biological activities, it could be of interest to develop methodologies giving access not only to the natural compounds but also to the corresponding non-natural and *ent*-14β-hydroxysteroids. Indeed, if the biological activities of natural 14β-hydroxysteroids were thoroughly studied and only few biological evaluations concerning non-natural and *ent*-14β-hydroxysteroids were reported, it will be the main reason for being the availability of the compounds of interest.[10]

In this context, we became interested in the development of diastereo-/enantioselective routes to natural and non-natural 14β-hydroxyandrostanes *via* Diels–Alder (DA) reactions calling for the B-cycle formation *ie* reaction between a diene **5** and a dienophile **6** bearing a β-hydroxy group at the ring junction. This approach seems at first glance trivial. Indeed, numerous steroids were already obtained *via* inter- or intramolecular DA-reactions, but surprisingly, the DA-approach was never reported for the synthesis of 14β-hydroxysteroids *via* the formation of the B-cycle (**Figure 2**).[11]

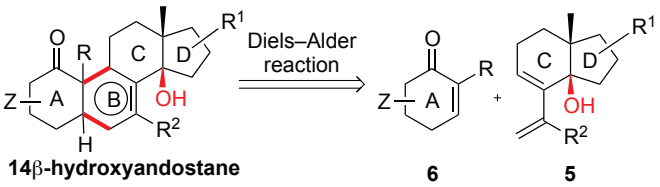

Figure 2. Retrosynthetic analysis for the synthesis of 14β-hydroxyandrostanes

Our strategy had to be highly selective for the following reason: the DA-reaction between a diene **5** and a dienophile **6** could afford four different isomers **7**-**10** resulting from *endo*/*exo* and concave/convex approaches. Moreover, it is well known that for DA-reactions, the formation of *endo*-adducts **7** and **8** is in general favored.[12] Natural 14β-hydroxysteroids can only result from an *exo*/convex approach, the other compounds being non-natural isomers. Therefore, our DA methodology should be highly diastereo/enantioselective to give either natural or non-natural 14β-hydroxysteroids (**Scheme 1**).

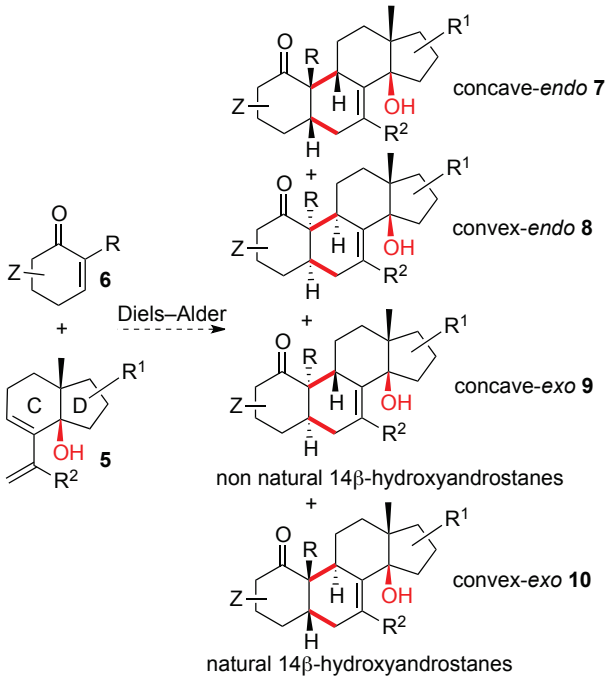

Scheme 1. Access to natural and non-natural 14β-hydroxysteroids *via* Diels–Alder reaction

RESULTS AND DISCUSSION

The DA approach was motivated by the fact that we had already developed efficient approaches to the racemic polyfunctionalized hydrindane **12** using either Halo-Michael-Aldol (HMA) or Morita–Baylis–Hillman (MBH) approaches, the starting material being 2-methyl-1,3-cyclopentanedione **11**. Hydrindane **12** represents a relevant substructure (C-D rings) of the compounds of interest (Scheme 2).[13]

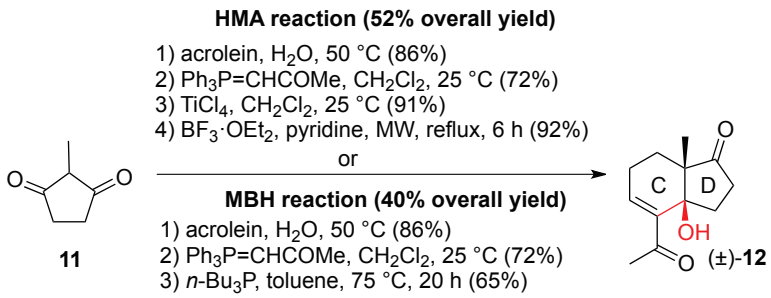

Scheme 2. Synthesis of hydrindane **12**

The hydrindane **12** was readily transformed into the bis-silyl enol ether **13** using conventional reaction conditions. Despite several trials, we were never able to isolate a mono silyl enol ether **14** or **15** (**Scheme 3**).

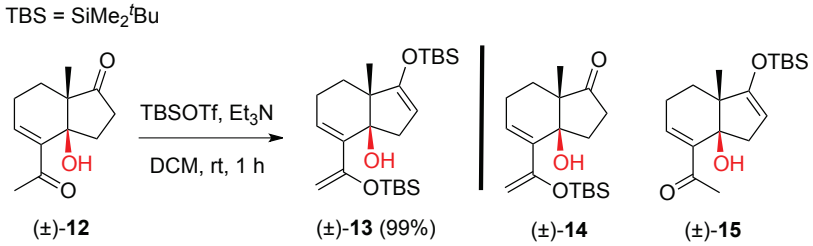

Scheme 3. Formation of bis-silyl enol ether **13**

The first DA-reaction was carried out with 2-methyl-2-cyclohexen-1-one **16** as a dienophile. At room temperature or by heating in high boiling point solvents, the starting material was recovered or degraded. Therefore, a Lewis acid activation had to be utilized to promote the progress of the reaction. Taking into account the results obtained by Corey *et al*. for the synthesis of steroids, we decided to use aluminium based Lewis acids.[14a,b] This choice was also motivated by the fact that de Groot *et al*. showed that the DA-reaction of 2-trimethylsilyloxy-1,3-butadiene with (*S*)-carvone delivered readily the corresponding DA-adduct in the presence of $EtAlCl_2$ and that in the presence of other Lewis acids the silyloxydiene was unstable.[14c]

For our first trial, trimethylaluminium (Me_3Al) was utilized as Lewis acid: no reaction took place (entry 1). With diethylaluminium chloride (Et_2AlCl; 20 mol%), *endo*-adduct **17** and *endo*-Michael adduct **18** were isolated in poor yield (7 and 5%) along with silyl ether **15** (23%) and starting material **13** (49%) (entry 2). When the reaction was carried out in the presence of 40 mol% Et_2AlCl and an excess dienophile (2.2 eq), the yield of *endo*-adduct **17** and *endo*-Michael adduct **18** increased (18 and 36%), but silyl ether **15** was still isolated in 17% yield (entry 3). Switching to ethylaluminium dichloride ($EtAlCl_2$; 20 mol%), the DA-reaction afforded *endo*-adduct **17** and *endo*-Michael adduct **18** in higher yields (21 and 31%), but silyl ether **15** was again isolated in 25% yield (entry 4). By increasing the amounts of $EtAlCl_2$ (40 mol%)

and dienophile (2.2 equiv), *endo*-adduct **17** and *endo*-Michael adduct **18** were respectively obtained in 8 and 65% yield (entry 5). Next, by increasing or decreasing the amount of Lewis acid, a yield drop for *endo*-adduct **17** and *endo*-Michael adduct **18** was observed (entries 6 and 7). In the presence of aluminium trichloride ($AlCl_3$), the formation of *endo*-adduct **17** and *endo*-Michael adduct **18** took also place but silyl ether **15** was again isolated in 18% yield (entry 8). In toluene, the yields dropped down (entry 9) and in acetonitrile, ethanol or DMF, no reaction occurred (entries 10-12) (**Table 1**).

From these results, we concluded that working in dichloromethane with an excess of dienophile (2.2 equiv) at low temperature (–78 °C) and using $EtAlCl_2$ (40 mol%) as Lewis acid, proved to be the optimal reaction conditions for our DA reaction. In this case, the *endo*-adduct **17** and the *endo*-Michael adduct **18** were isolated in respectively 8 and 65% yield. The relative configurations of the latter were secured by X-ray analysis.[15]

Table 1. Screening of conditions to achieve the Lewis acid catalyzed Diels–Alder reaction

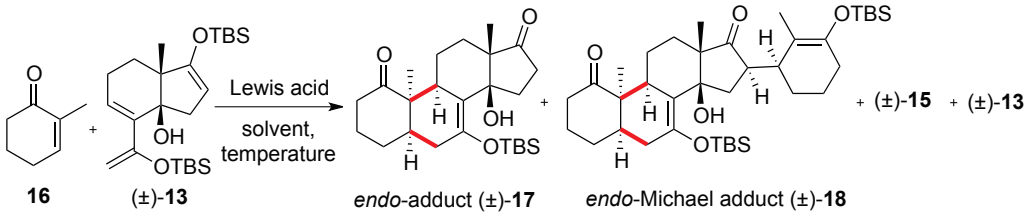

16 (±)-**13** *endo*-adduct (±)-**17** *endo*-Michael adduct (±)-**18**

Entry	Dienophile (equiv.)	Diene (equiv.)	Catalyst	Solvent Temperature	**17** (%)	**18** (%)	**15** (%)	**12** (%)	**13** (%)
1	1	1	Me_3Al (20 mol%)	CH_2Cl_2, –78 °C					99
2	1	1	Et_2AlCl (20 mol%)	CH_2Cl_2, –78 °C	7	5	23		49
3	2.2	1	Et_2AlCl (40 mol%)	CH_2Cl_2, –78 °C	18	36	17		
4	1	1	$EtAlCl_2$ (20 mol%)	CH_2Cl_2, –78 °C	21	31	25		
5	2.2	1	$EtAlCl_2$ (40 mol%)	CH_2Cl_2, –78 °C	8	65			
6	2.2	1	$EtAlCl_2$ (20 mol%)	CH_2Cl_2, –78 °C	11	38			
7	2.2	1	$EtAlCl_2$ (80 mol%)	CH_2Cl_2, –78 °C	7	53	12		
8	2.2	1	$AlCl_3$ (40 mol%)	CH_2Cl_2, –78 °C	10	51	18		
9	2.2	1	$EtAlCl_2$ (40 mol%)	toluene, –78 °C		15	26		27
10	2.2	1	$EtAlCl_2$ (40 mol%)	MeCN, –40 °C				99	
11	2.2	1	$EtAlCl_2$ (40 mol%)	EtOH, –78 °C					99
12	2.2	1	$EtAlCl_2$ (40 mol%)	DMF, –40 °C					99

Thus, the obtaining of *endo*-adducts was in good accordance with the well-known DA-rules.[12] However, our DA-reaction was carried out using Lewis acid activation. At this stage it was reasonable to suggest that our Diels–Alder reaction occurred through a stepwise mechanism *via* the formation of the Mukaiyama–Michael **19** intermediate, the latter evolving toward the *endo*-adduct **20**. However, later on, DFT calculations allowed us to propose a new mechanism (see page 13). The latter was not isolable and evolved according to two different pathways: either by hydrolysis of the C16–C17 enoxy-silane bond to give the *endo*-adduct **17**, or *via* a 1,4-addition with the excess of dienophile to yield the *endo*-Michael adduct **18**. Thus it was reasonable to postulate that the cyclohexanone carbonyl group can approach the vinylogous silyl enol ether (±)-**13** on the top face without significant steric hindrance, the bottom face being more sterically hindered. Our DA-reaction proved to be highly diastereoselective because only one *endo*-isomer was isolated among the four possible (**Scheme 4**).

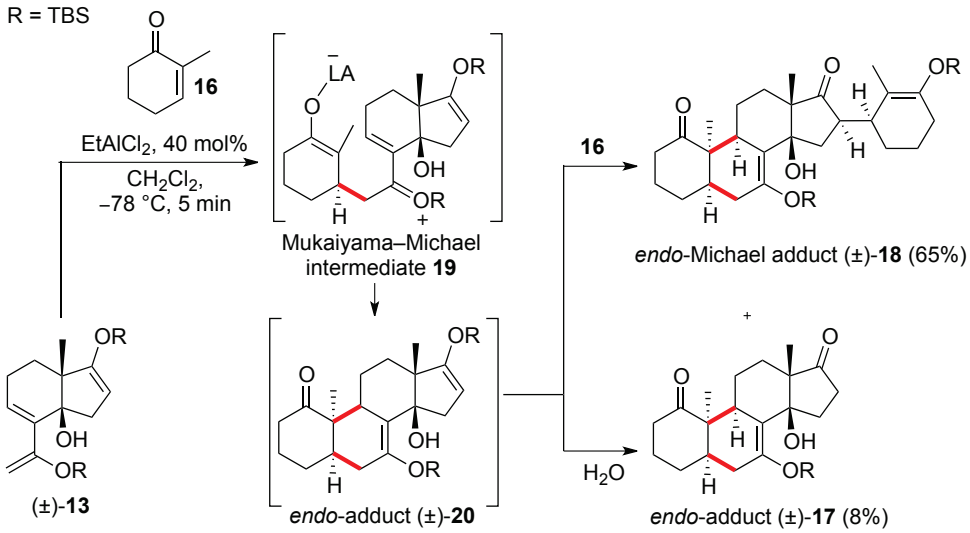

Scheme 4. Synthesis of *endo*-Michael adduct **18** and *endo*-adduct **17**

At this stage another question arose concerning the formation of *endo*-Michael adduct **18**: does the Michael addition take place after the DA-reaction between the diene **13** and the dienophile (route A) or does the Michael addition between diene **13** and the dienophile take place before the DA-reaction (formation of compound **21**; route B) (**Scheme 5**)?

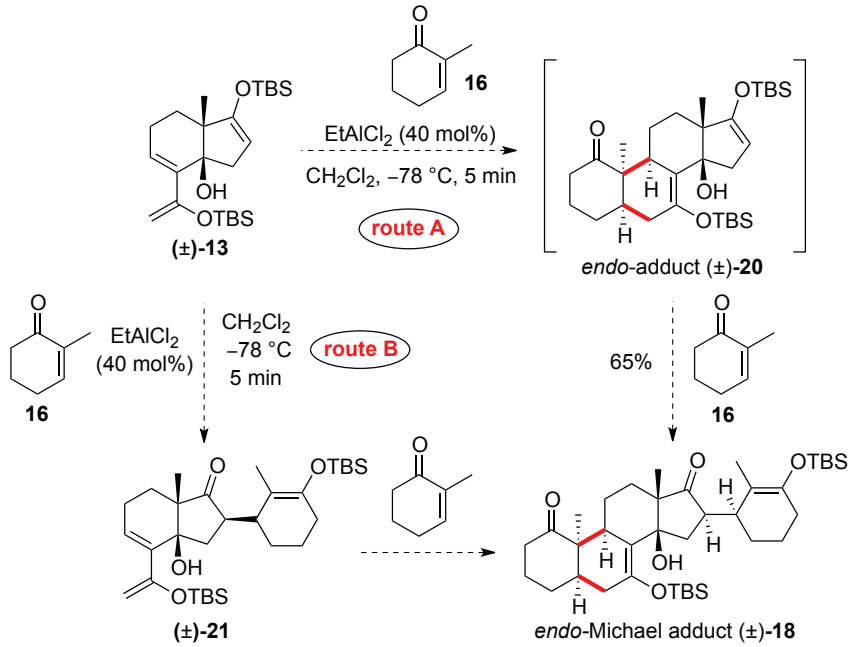

Scheme 5. When does the Michael addition take place?

To answer this question, diene **13** was treated under the optimum reaction conditions used for the DA-reaction. Under these reaction conditions [$EtAlCl_2$ (40 mol%), –78 °C], compound **15** was isolated indicating that the dienoxy-silane was first hydrolyzed. Accordingly the latter proved to be more reactive compared to the 5-membered ring enoxy-silane (**Scheme 6**).

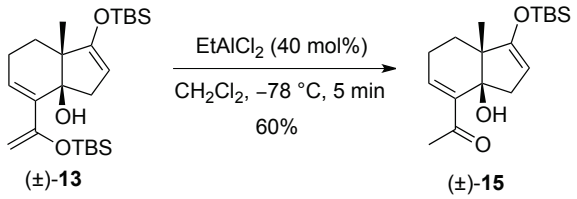

Scheme 6. Regioselective deprotection of hydrindane **13**

Therefore, it was reasonable to claim that the formation of compound **20** took place initially (route A favored), the latter evolving either by hydrolysis (formation of the *endo*-adduct **17**) or by Michael addition with the dienophile (formation of the *endo*-Michael adduct **18**).

Our first results have shown that in the case of a Lewis acid activation, the sole *endo*-adducts characterized by a *cis* α A/B ring junction were formed. However, natural 14β-hydroxyandrostanes are characterized by a *cis* β A/B ring junction. Therefore, if we want to use our DA-methodology to get natural 14 β-hydroxyandrostanes, we have to develop a new strategy giving exclusively access to DA-adducts resulting from an *exo*-approach between the diene and the dienophile.

In this context, Jung *et al*. reported that when a DA-reaction was performed between diene **22** and 2-methyl-2-cyclohexen-1-one **16**, the *endo* **23**/*exo* **24** adducts ratio was 2.5/1. However, when the reaction was carried out with the β-ketoester **25** which can be considered as an activated dienophile, the *endo* **26**/*exo* **27** adducts ratio was 1.3/1.[16] This indicated clearly that the electron-withdrawing group was the directing group promoting the formation of an *exo*-adduct. Note that activation of the DA-reaction by a Lewis acid was necessary in both cases (**Scheme 7**).

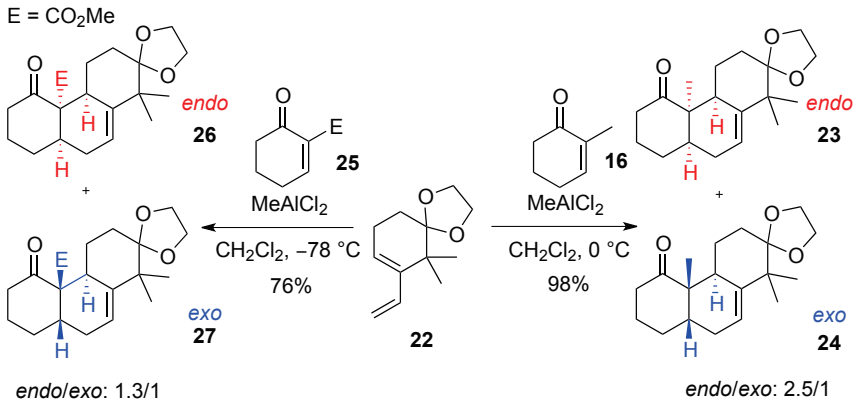

Scheme 7. Diels Alder reaction with β-ketoester **25** and diene **22** according to Jung *et al*.[16]

Therefore, compound **28** was first utilized as an activated dienophile. We began using the reaction conditions described by Jung *et al*., namely activation by a Lewis acid. However, under activation with $EtAlCl_2$, decomposition of the reaction mixture occurred. Thereafter, the reaction was carried out in refluxing toluene for 24 h leading to the *exo*-adduct **29** isolated in 14% yield (**Scheme 8**).

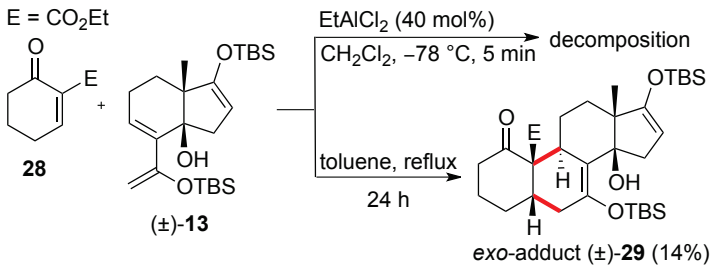

Scheme 8. Synthesis of *exo*-adduct **29** under thermal activation

To improve the formation of *exo*-adduct **29**, we used high pressure activation for our DA-reaction.[17] Thus, by carrying out the DA-reaction under 0.9 GPa, the *exo*-adduct **29** was isolated in 82% yield along with another adduct **30** isolated in 12% yield. The structure of the latter corresponds to the *endo*-adduct because, until now, we never observed adducts resulting from *exo*- or *endo*-concave approaches. Thus,

our DA-reaction was highly diastereoselective, the relative configurations of *exo*-adduct **29** being secured by X-ray structure analysis (**Scheme 9**).[18]

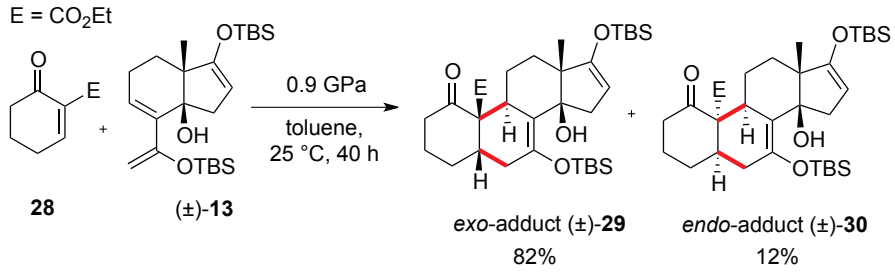

Scheme 9. Diastereoselective synthesis of *exo*-adduct **29** under high pressure activation

We also studied our DA-reaction between diene **13** and dienophile **28** using water as a solvent. The interest of such a study lies in the properties of the reaction medium. Indeed, the use of water as solvent can allow an increase in the rate and selectivity of the reaction by hydrophobic and hydrogen bonding effects. Under these conditions, the DA-reaction afforded the *exo*-adduct **29** in 22% yield along with compound **15** corresponding to the regioselective hydrolysis of dienoxy-silane **13** and unreacted diene **13** (**Scheme 10**).

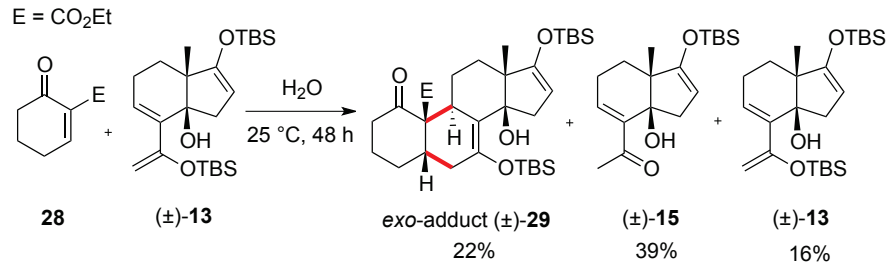

Scheme 10. Synthesis of *exo*-adduct **29** using water as solvent

At this stage, other dienophiles bearing a functional group, precursor of a 3β-hydroxy group (steroid numbering), were utilized as for example compounds **31** and **32** which were readily available according to literature procedures. The DA-reaction took place again affording exclusively the corresponding *exo*-adducts **33** and **34** in 78 and 85% yields (**Scheme 11**). The relative configurations of *exo*-adduct **33** were secured by X-ray analysis.[19]

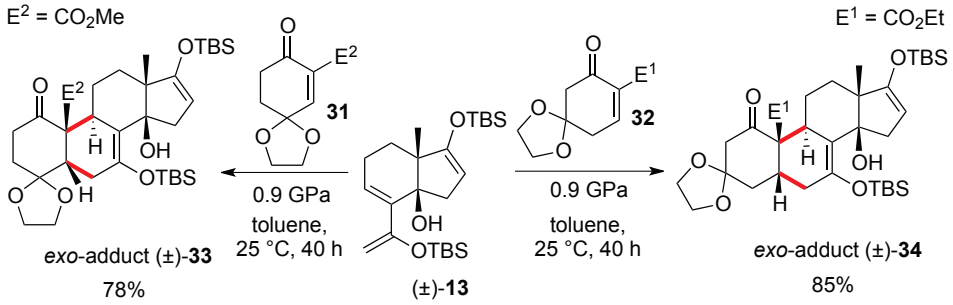

Scheme 11. Diastereoselective synthesis of *exo*-adducts **33** and **34**

Up to now, the DA-adducts had been obtained as racemic mixtures. Next, our goal was to set-up an asymmetric version of the DA-reaction. Several possibilities were considered: either to use a chiral Lewis acid or a chiral diene or a chiral dienophile. Firstly, we chose to use a chiral dienophile, namely (*R*)-carvone **35**. The latter is commercially available, cheap and is derived from the chiral pool. Apparently, this choice may appear to be unreasonable. Indeed, we had shown that the DA-reaction of 2-methyl-2-cyclohexen-1-one **16** with diene **13** afforded exclusively *endo*-adducts. Despite these results, the DA-reaction between (*R*)-carvone **35** and diene **13** was carried out under Lewis acid activation. Surprisingly, *exo*-adduct (–)-**36** and *endo*-Michael adduct (–)-**37** were isolated in respectively **37** and 39% yield (ee>98%)! The absolute configurations of the latter were secured by X-ray structure analysis. The DA-reaction was also carried out with (*S*)-carvone **38** as dienophile. The enantiomers (+)-**36** and (+)-**37** of the previous adducts were isolated in identical yields with ee> 98%.[20] These compounds represent in fact *ent*-14β-hydroxysteroids. At this stage it has to be emphasized that only five steps were necessary to get the compounds of interest starting from an achiral compound *ie* methyl-2-cyclopentane-1,3-dione. Thus, our synthetic route represents, to the best of our knowledge, one of the fastest accesses to *ent*-14β-hydroxysteroids (**Scheme 12**).

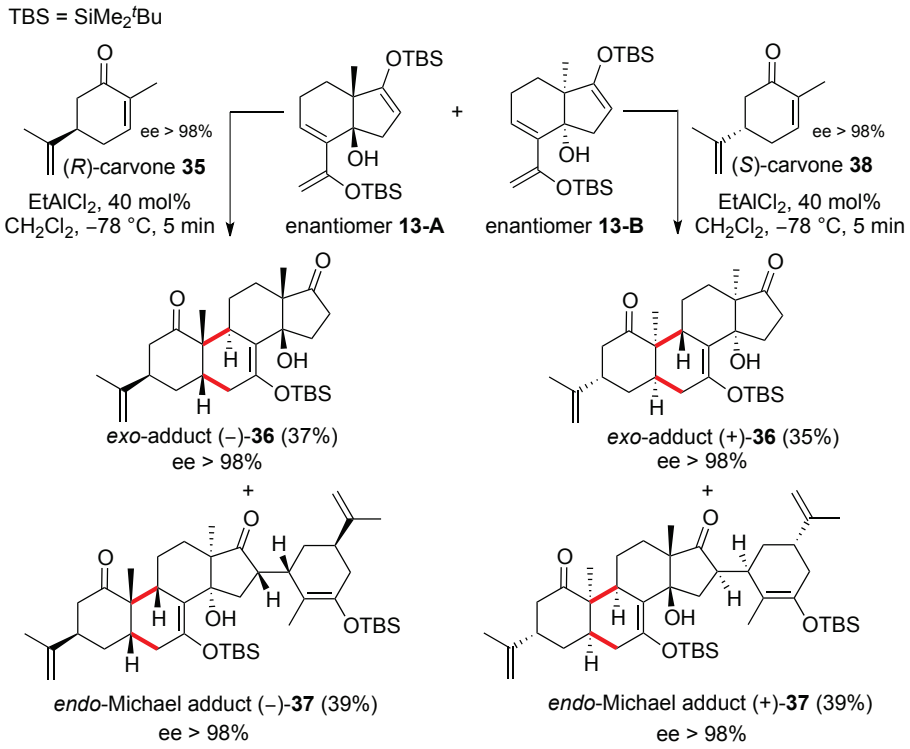

Scheme 12. Diels–Alder reaction under parallel chemodivergent kinetic resolution control

These results were completely unexpected and clearly indicated that the two enantiomers **13**-**A** and **13**-**B** of the racemic diene **13** reacted differently with (*R*)- or (*S*)-carvone. In each case, the DA-adducts **36** and **37** were neither isomers nor enantiomers of each other. Thus, it was reasonable to claim that the DA–reaction took place under a parallel, chemodivergent kinetic resolution control (*vide infra*).[21]

The results obtained with (*R*)- or (*S*)-carvone, prompted us to synthesize different functionalized chiral dienophiles **39**-**41** bearing a potential precursor of a 3β-hydroxy group (steroid numbering).[22] Unfortunately, complex reaction mixtures were obtained when running the DA-reaction with diene **13** under Lewis acid activation (**Scheme 13**).

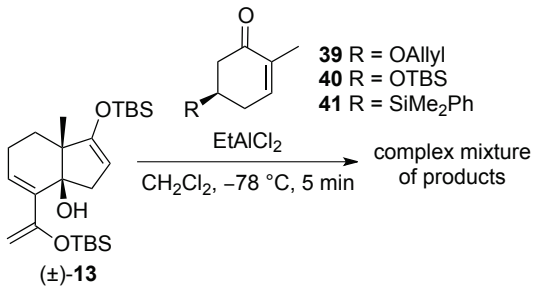

Scheme 13. Diels–Alder reaction with chiral dienophiles **39**, **40**, **41** and diene **13**

To extend the scope of our methodology, we became interested in a DA-reaction implementing new polyfunctionalized dienes. For example, hydrindane **45** was obtained as follow: starting from chiral

Hajosh–Parrish ketone (+)-**42** (ee>98%),[23] ketoaldehyde (+)-**43** was obtained according to literature procedures. A Wittig reaction afforded the α,β-unsaturated ketone (+)-**44** which was submitted either to HMA or MBH usual reaction conditions. Unfortunately, the desired polyfunctionalized hydrindane (–)-**45** was not isolated. However under high pressure reaction conditions, the desired compound (–)-**45** was readily obtained and transformed into diene (+)-**46** (**Scheme 14**).

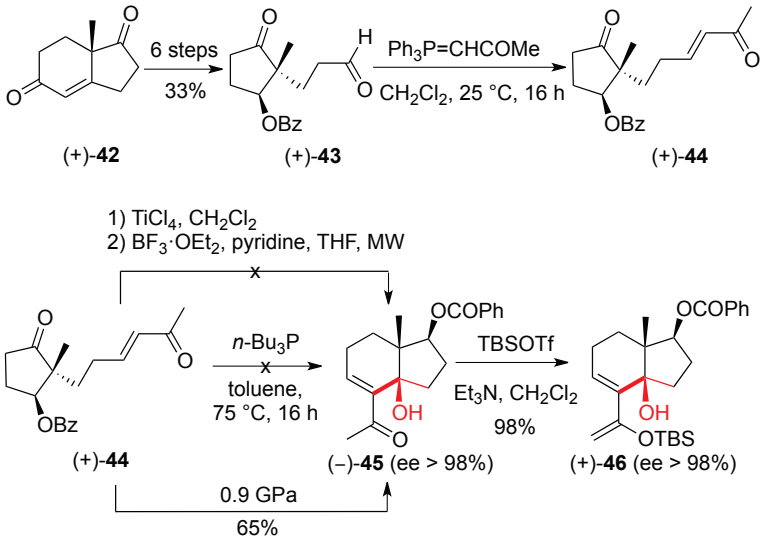

Scheme 14. Synthesis of enantiomerically pure hydrindane **46**

The DA-reaction was carried out with diene (+)-**46** and different activated dienophiles **28**, **31**, **32** and **47** under high pressure activation to yield the corresponding *exo*-Diels–Alder adducts **48-51** in high yields and with high diastero/enantioselectivities (ee > 98%) (**Scheme 15**).[24]

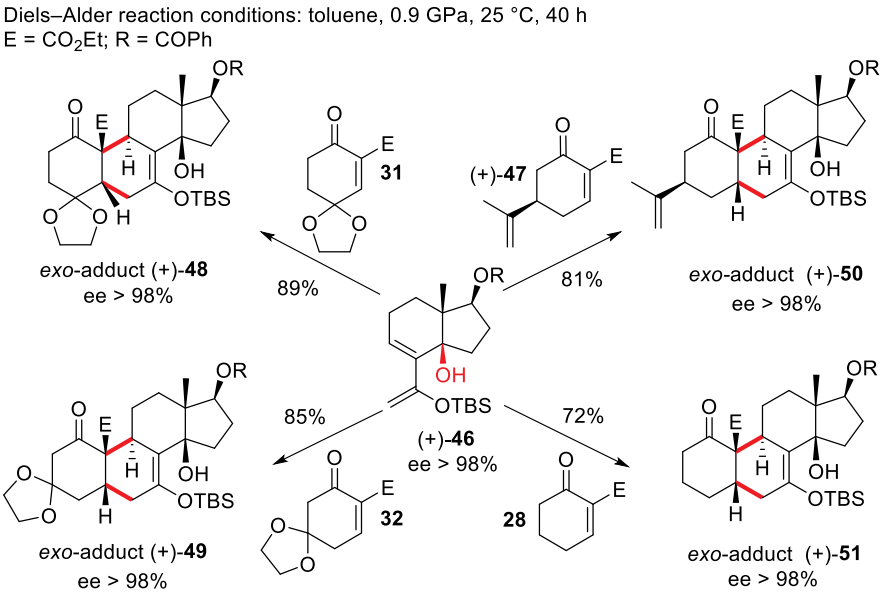

Scheme 15. Synthesis of enantiomerically pure 14β-hydroxyandrostanes

The availability of diene (+)-**46** is of interest because the resulting 14β-hydroxyandrostanes **48**-**51** are now bearing up to 5 different functional groups in positions 1, 3, 7, 10 and 17. Thus, further selective synthetic transformations should be easier to achieve.

To bring more highlights to the origin of the selectivities encountered for our DA-reactions [DA-adducts and Diels–Alder–Michael (DAM)-adducts], density functional theory (DFT) calculations at B3LYP/6-31G* level using simplified model substrates were undertaken.[25] We had to rationalize the four interesting phenomena regarding the parallel kinetic resolution observed for the DA-reaction: (i) DA-*exo* (–)-**36** was selectively obtained from enantiomer **13-A**; (ii) DAM-*endo* (–)-**37** was selectively obtained from enantiomer **13-B**; (iii) DA-*exo* (–)-**36** was not converted into the corresponding DAM; (iv) DA-*endo* was easily converted into the corresponding DAM-*endo* (–)-**37**.

Firstly, we categorized the patterns of transition states (TS) in the DA–reaction between (*R*)-carvone and diene **52-A**.

For enantiomer **52-A**, there are four types of TS, which have concave-*endo* (A-type: **53-TS**), concave-*exo* (B-type: **54-TS**), convex-*endo* (C-type: **55-TS**), and convex-*exo* (D-type: **56-TS**) configurations (**Scheme 16**).

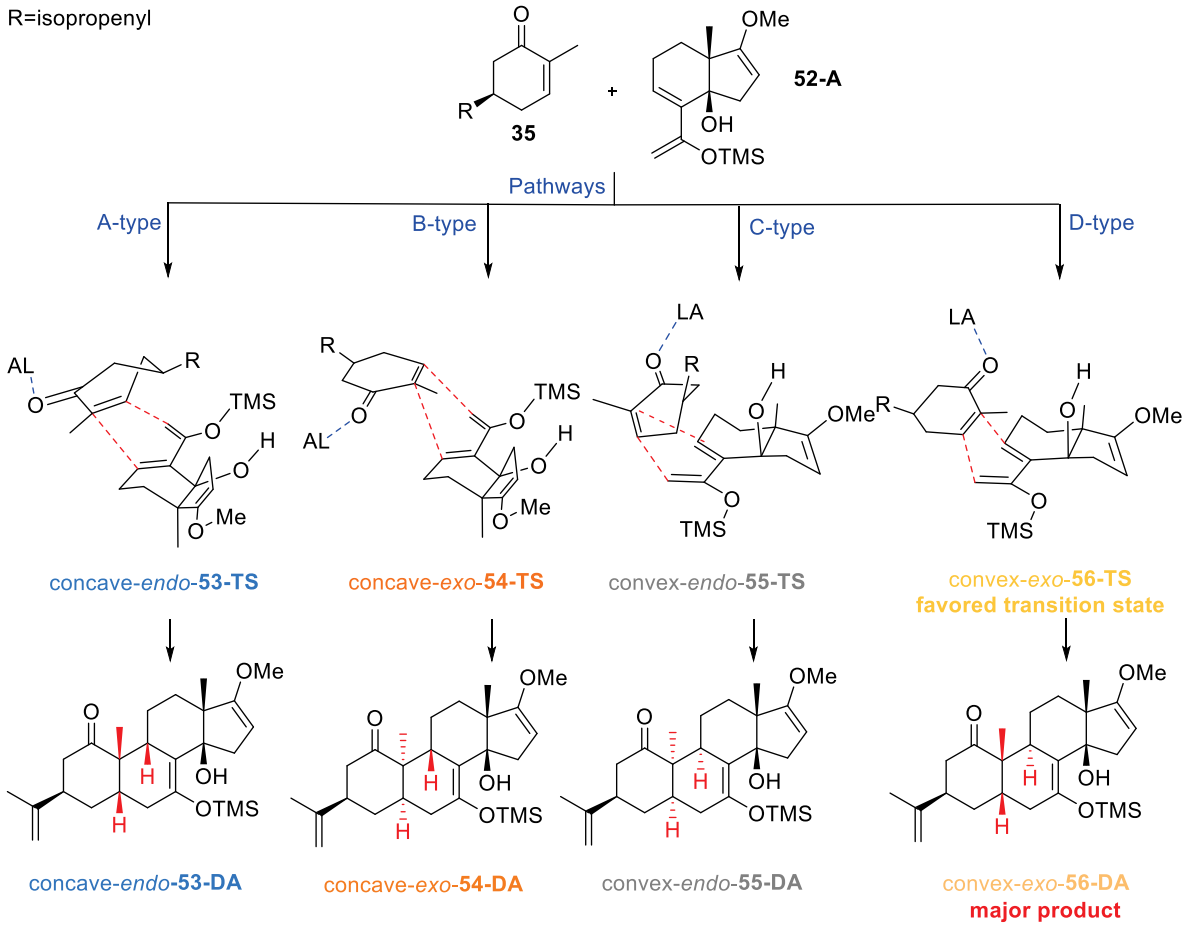

Scheme 16. Possible transition states to form concave/convex and *exo*/*endo* DA-adducts **53**-**56**

We examined the reason why convex-*exo*-**56**-**DA** was selectively obtained using the DA-reaction between (*R*)-carvone and diene **52-A** as model. The reaction coordinates of the DA-reaction affording concave-*endo*-**53**-**DA**, concave-*exo*-**54**-**DA**, and convex-*endo*-**55**-**DA** and convex-*exo*-**56**-**DA** *via* the TSs A, B, C and D-type were depicted in **Figure 3**.

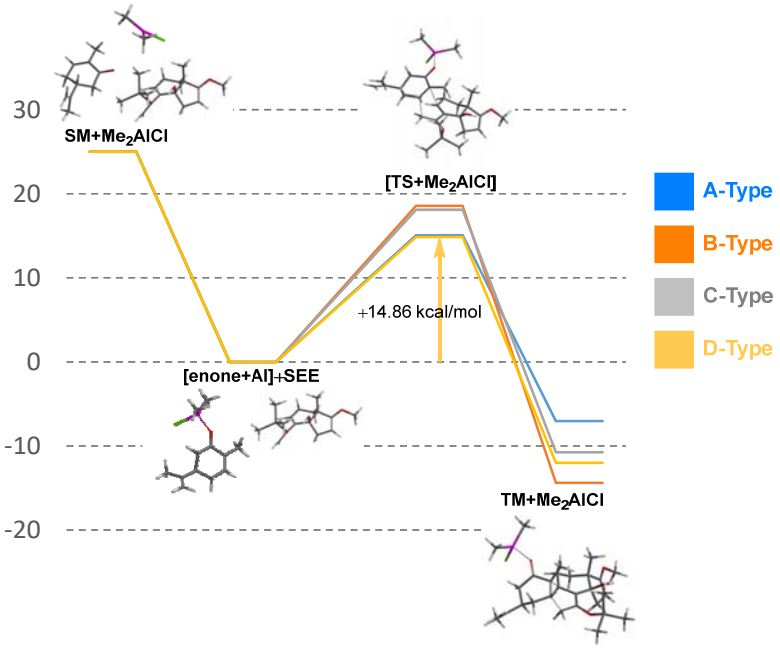

Pathway Type	[SM+Me_2AlCl]	[enone+Al]+SEE	[TS+Me_2AlCl]	ΔE_{TS}	[TM+Me_2AlCl]
A type	25.00	0.00	15.07	0.21	−7.04
B type	25.00	0.00	18.57	3.71	−14.38
C type	25.00	0.00	18.16	3.30	−10.74
D type	25.00	0.00	14.86	0.00	−12.01

Figure 3. Reaction coordinates to form DA-adducts **53**-**56**

We found that the TS energy of convex-*exo*-**56**-TS was very low (14.86 kcal/mol) compared to the concave-*endo*-**53**-TS, concave-*exo*-**54**-TS, and convex-*endo*-**55**-TS energies (15.07, 18.57 and 18.16 kcal/mol). Therefore, we assumed that the favored TS for the DA-reaction between (*R*)-carvone and diene **52-A** was the convex-*exo*-**56**-TS.

Moreover, differences in the activation energy derived from each activation energy ([TS+Me_2AlCl] – ([enone+Al]+SEE)) corresponding to the relative activation energies for B-type-TS (concave-*exo*-**54**-TS; $\Delta E_{TS(B\text{-}D)}$ = 3.71 kcal/mol) and C-type-TS (convex-*endo*-**55**-TS; $\Delta E_{TS(C\text{-}D)}$ = 3.24 kcal/mol) were so large (over 2 kcal/mol) compared to those for A-type-TS (concave-*endo*-**53**-TS; $\Delta E_{TS(A\text{-}D)}$ = 0.21 kcal/mol) and D-type-TS ($\Delta E_{TS(D\text{-}D)}$ = 0.00 kcal/mol). Therefore, the formation of concave-*exo*-**54**-TS and convex-*endo*-**55**-TS was kinetically prohibited. On the other hand, the TS energies of concave-*endo*-**53**-TS and convex-*exo*-**56**-TS were approximately equal.

However, the activation energy of convex-*exo*-**56-**DA (D-type pathway) was enormously lower compared to the activation energy of concave-*endo*-**53-DA** (A-type pathway) by ~5 kcal/mol. Therefore, convex-*exo*-**56-DA** was exclusively formed under the thermodynamic reaction conditions.

Based on the above analysis, it was concluded that concave-*endo*-**53-**DA and convex-*exo*-**56-DA** were kinetically selected during the reaction process. Additionally, it was also noted that convex-*exo*-**56-DA** was not only kinetically but also thermodynamically selected for the DA-reaction during the reaction process.

For enantiomer **52-B**, there were also four types of TS which have ent-concave-*endo* (E-type: **57-**TS), ent-concave-*exo* (F-type: **58-**TS), ent-convex-*endo* (G-type: **59-**TS and ent-convex-*exo* (H-type: **60-**TS) configurations (**Scheme 17**).

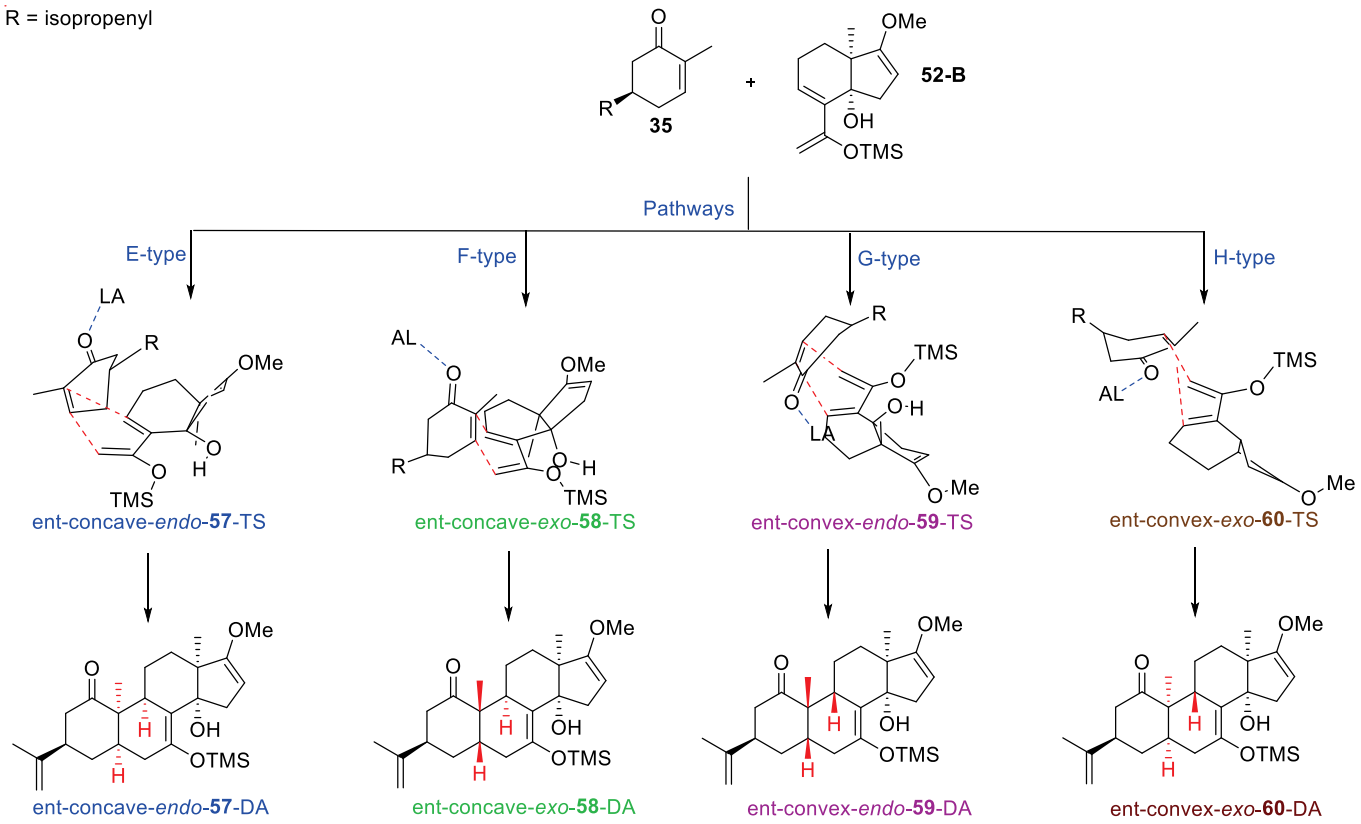

Scheme 17. Possible transition states to form concave/convex and exo/endo DA-adducts **57-60**

The reaction coordinates of the DA-reaction affording concave-*endo*-**57-DA**, concave-*exo*-**58-DA**, convex-*endo*-**59-DA** and convex-*exo*-**60-DA** *via* the transition states E, F, G and H types were depicted in **Figure 4**.

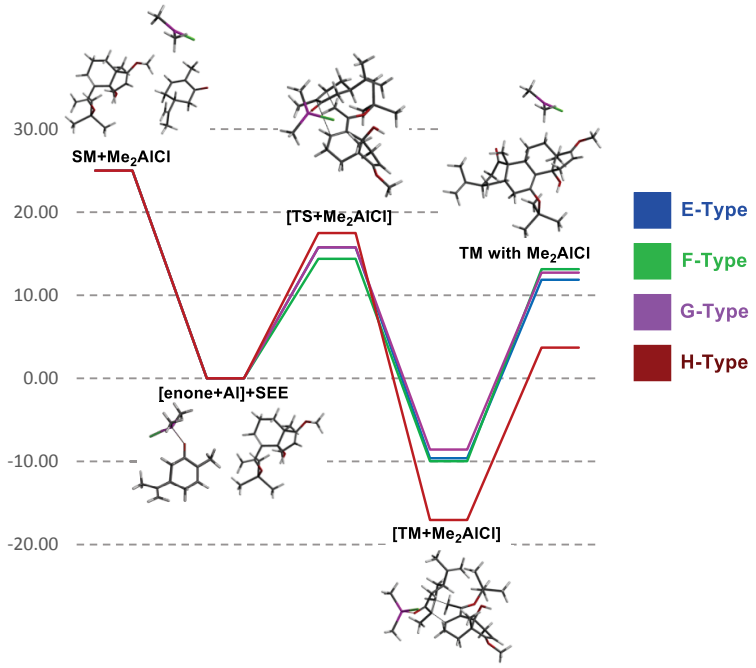

Pathway Type	[SM+Me_2AlCl]	[enone+Al]+SEE	[TS+Me_2AlCl]	ΔE_{TS}	[TM+Me_2AlCl]	TM with Me_2AlCl
E type	25.00	0.00	15.77	0.00	–9.61	11.86
F type	25.00	0.00	14.38	–1.39	–9.97	13.13
G type	25.00	0.00	15.77	0.00	–8.57	12.72
H type	25.00	0.00	17.49	1.72	–17.04	3.70

Figure 4. Reaction coordinates to form DA-adducts **57**-**60**

It resulted that the TS energy for ent-convex-*exo*-**60**-TS was very high (17.49 kcal/mol) compared to ent-concave-*endo*-**57**-TS (15.77 kcal/mol), ent-concave-*exo*-**58**-TS (14.38 kcal/mol) and ent-convex-*endo*-**59**-TS (15.77 kcal/mol). Therefore, ent-convex-*exo*-**60**-TS should be the most unstable TS among all four TSs.

On the other hand, the activation energy difference derived from each activation energy ([TS+Me_2AlCl] – ([enone+Al]+SEE)) corresponding to the relative activation energy for H-type-TS (ent-convex-*exo*-**60**-TS; $\Delta E_{TS(H\text{-}F)}$ = 3.11 kcal/mol) was over 2 kcal/mol compared to E-type (ent-concave-*endo*-**57**-TS-; $\Delta E_{TS(E\text{-}F)}$ = 1.39 kcal/mol), F-type (ent-concave-*exo*-**58**-TS; $\Delta E_{TS(F\text{-}F)}$ = 0.00 kcal/mol) and G-type (ent-convex-*endo*-**59**-TS; $\Delta E_{TS(G\text{-}F)}$ = 1.39 kcal/mol). Therefore, formation of convex-*exo*-**60**-TS was kinetically prohibited.

It also came out from the DFT calculations that the TS energies of ent-concave-*endo*-**57**-TS (15.77 kcal/mol), ent-concave-*exo*-**58**-TS (14.38 kcal/mol), ent-convex-*endo*-**59**-TS (15.77 kcal/mol) were very close as well as the activation energies of concave-*endo*-**57-DA** with Me_2AlCl (11.86 kcal/mol), concave-*exo*-**58-DA** with Me_2AlCl (13.13 kcal/mol) and convex-*endo*-**59-DA** with Me_2AlCl (12.72 kcal/mol).

Thus, the activation energy differences were too low to account for the experimental results and further considerations were required to explain the selective formation of DAM-adducts.

We used 2-methyl-2-cyclohexenone **16** as dienophile and diene **61-B** to carry out the DFT calculation accounting for the formation of concave-*endo*-**62-DAM** (E'-type), concave-*exo*-**63-DAM** (F'-type), convex-*endo*-**64-DAM** (G'-type) and convex-*exo*-**65-DAM** (H'-type) (**Scheme 18**).

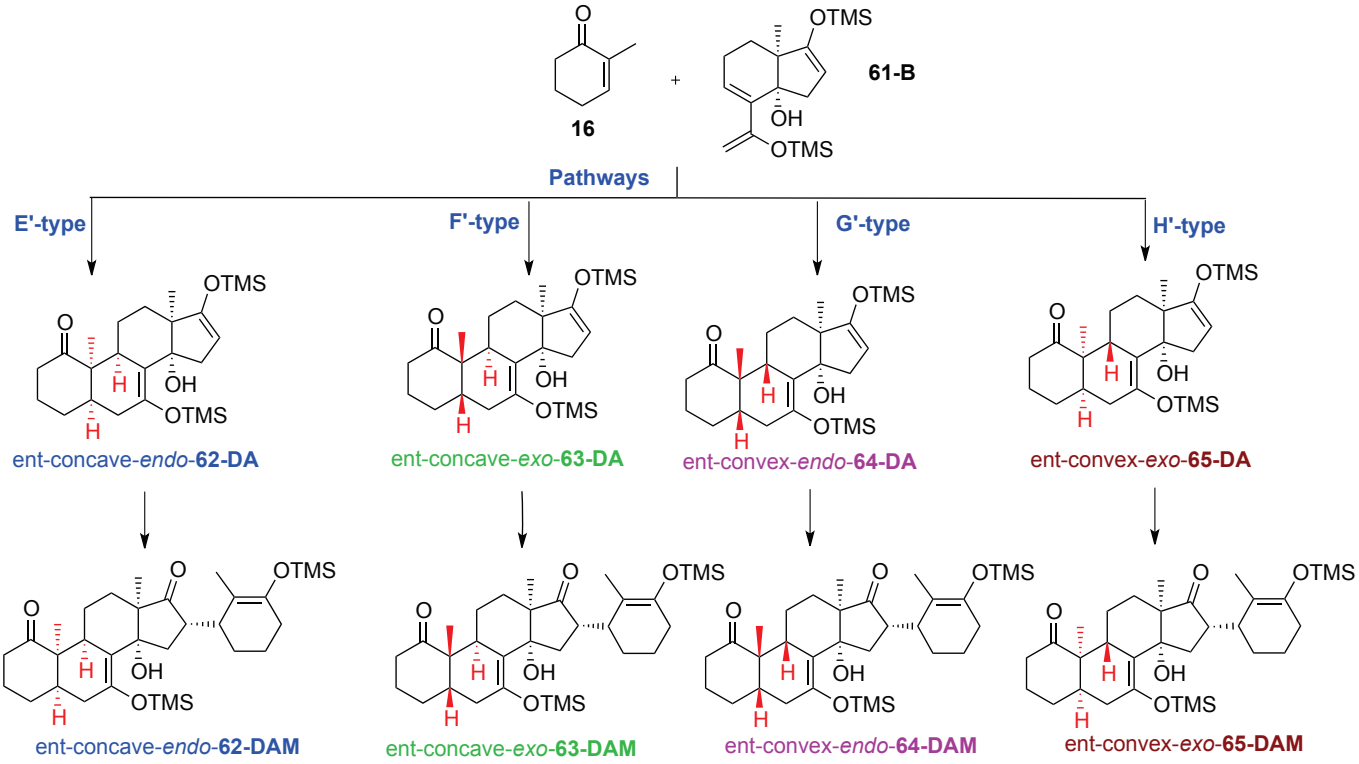

Scheme 18. Possible pathways to form concave/convex and exo/endo DAM-adducts **62-65**

To provide a reasonable answer to the above concerns, we envisioned a new reaction pathway. First, a transmetallation reaction of **62-65-DA** adducts with Me_2AlCl could afford aluminum enolates **62-65-Int-I**.[26] Afterwards, a conjugate addition *via* a six-membered cyclic transition state (TS2) with 2-methyl-2-cyclohexenone **16** could promote the formation of the Michael addition product **62-65-Int-II**. The latter could be converted into its *O*-bound aluminium enolates **62-65-Int-III**, evolving toward the desired product **62-65-DAM** through a transmetallation reaction with TMSCl (**Scheme 19**).

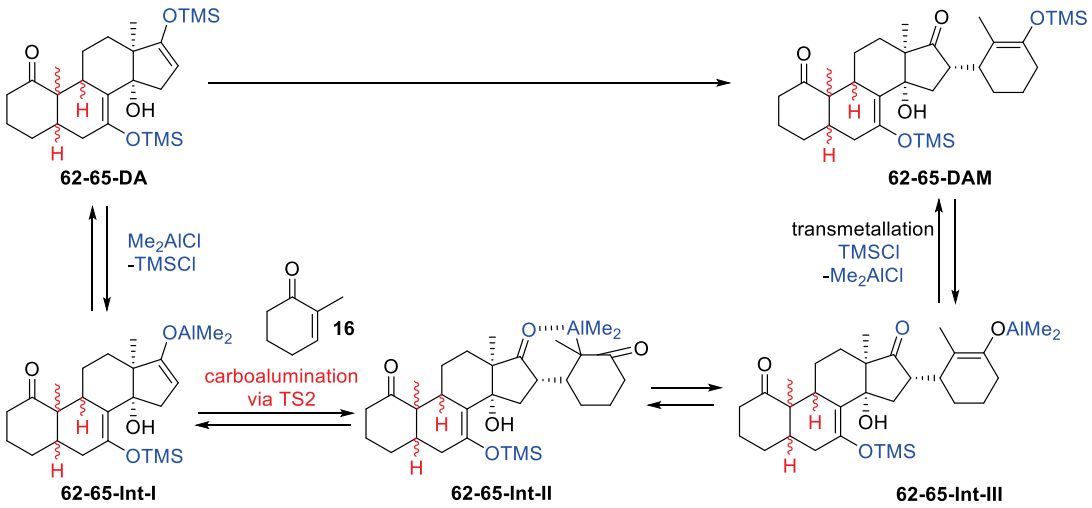

Scheme 19. Reaction pathway accounting for the formation of DAM adducts

The reaction coordinates of the Michael addition reaction affording E'-type Michael adduct (ent-concave-*endo*-**62-DAM**) *via* the transition state E'-type-TS2, F'-type Michael adduct (ent-concave-*exo*-**63-DAM**) *via* F'-type-TS2, G'-type Michael adduct (ent-convex-*endo*-**64-DAM**) *via* G'-type-TS2, and H'-type Michael adduct (ent-convex-*exo*-**65-DAM**) *via* H'-type-TS2 were depicted in **Figure 5**.

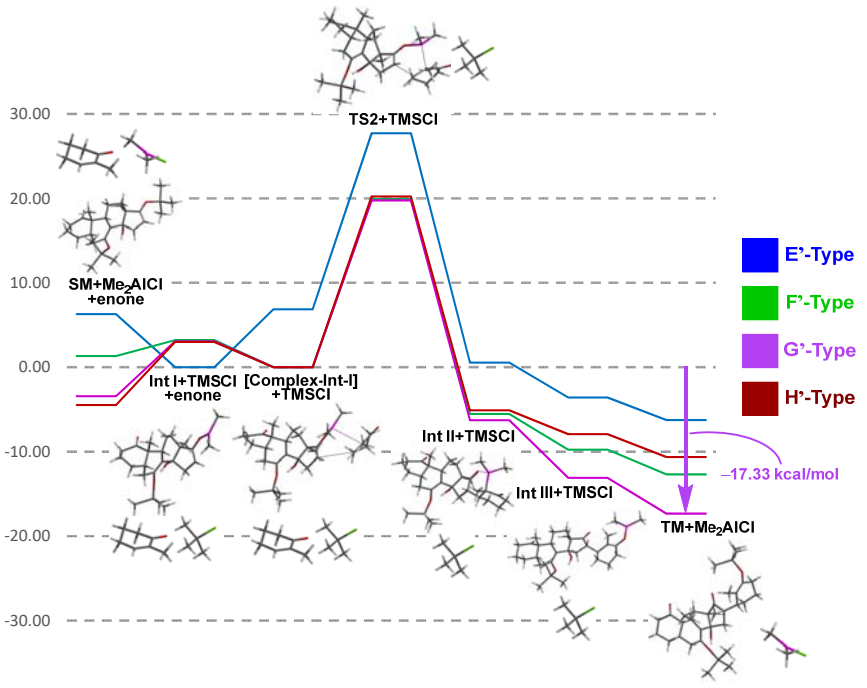

Pathway Type	SM+Me_2AlCl +enone	Int-I+TMSCl +enone	[Complex-Int-I] +TMSCl	TS2+TMSCl	Int-II+TMSCl	Int-III+TMSCl	TM with Me_2AlCl
E' type	6.28	0.00	6.86	27.72	0.54	–3.59	–6.26
F' type	1.32	3.21	0.00	19.90	–5.54	–9.76	–12.69
G' type	–3.44	3.07	0.00	19.76	–6.27	–13.10	–17.33
H' type	–4.47	2.99	0.00	20.23	–5.11	–7.93	–10.64

Figure 5. Reaction coordinates to form DAM-adducts **62-65**

First of all, we had already shown that the reaction pathway leading to ent-convex-*exo*-**60-DA** adduct was kinetically prohibited because the activation energy required for the DA-reaction was too high. Therefore, the Michael addition reaction affording ent-convex-*exo*-**65-DAM** was not considered.

On the other hand, the difference of activation energies between E'-type-TS2+TMSCl and F'-type-, G'-type-, and H'-type-TS2+TMSCl is over 7 kcal/mol. Therefore, the formation of E'-type-TS2+TMSCl is kinetically prohibited. Furthermore, the TS energy of G'-type-TS2 (19.76 kcal/mol) is lower than that of F'-type-TS2 (19.90 kcal/mol). However, the difference of these TS energies (0.14 kcal/mol) was not satisfactory to rationalize the high selectivity of our DAM-reaction. Therefore, we had to reconsider the origin of the selectivity accounting for the formation of F'-type or G'-type Michael adducts.

Focusing on the DAM adducts stability, the energy of G'-type Michael adduct (convex-*endo*-**64-DAM**: −17.33 kcal/mol)) was sufficiently lower compared to that of F'-type Michael adduct (concave-*exo*-**63-DAM**: −12.69 kcal/mol) by ~ 4.6 kcal/mol: hence G'-type Michael adduct (convex-*endo*-**64-DAM**) should be exclusively formed under thermodynamic reaction conditions. By accounting the solvation energy (using the SM8 solvation model) for the transition states of DA reaction and the products in dichloromethane (ε = 9.1), it was assumed that all the DA reactions to afford DA-adducts **57-60** except for DA reaction through TS **60-DA** are reversible under the reaction conditions. (Reverse activation energy for TS **57-DA** (direction for forming E-type SM from the DA-adduct): 25.38 kcal/mol (non-solvation) => 21.44 kcal/mol (solvation), Reverse activation energy for TS **58-DA** (direction for forming F-type SM from the DA-adduct): 24.35 kcal/mol (non-solvation) => 19.81 kcal/mol (solvation), Reverse activation energy for TS **59-DA** (direction for forming G-type SM from the DA-adduct): 24.34 kcal/mol (non-solvation) => 17.92 kcal/mol (solvation), Reverse activation energy for TS **60-DA** (direction for forming H-type SM from the DA-adduct): 34.53 kcal/mol (non-solvation) => 30.59 kcal/mol (solvation))

Based on the above analysis, we concluded that G'-type Michael adduct (convex-*endo*-**DAM**) was not only kinetically but also thermodynamically selected during the DAM reactions.

Therefore, it was reasonable to postulate that DAM adduct (−)-**37** was selectively obtained starting from (*R*)-carvone **35** and (−)-silyl enol ether ((−)-**12-B**).

Finally we investigated the reason why D'-type DA adduct (convex-*exo*-**66-DA**) was not converted into the corresponding Michael adduct (convex-*exo*-**67-DAM**) although G'-type DA adduct (convex-*endo*-**64-DA**) was easily converted into the corresponding Michael adduct (convex-*endo*-**64-DAM**). The DFT calculations were made by using the model substrate dienes (+)-**61-A** and (−)-**61-B** (**Scheme 20**).

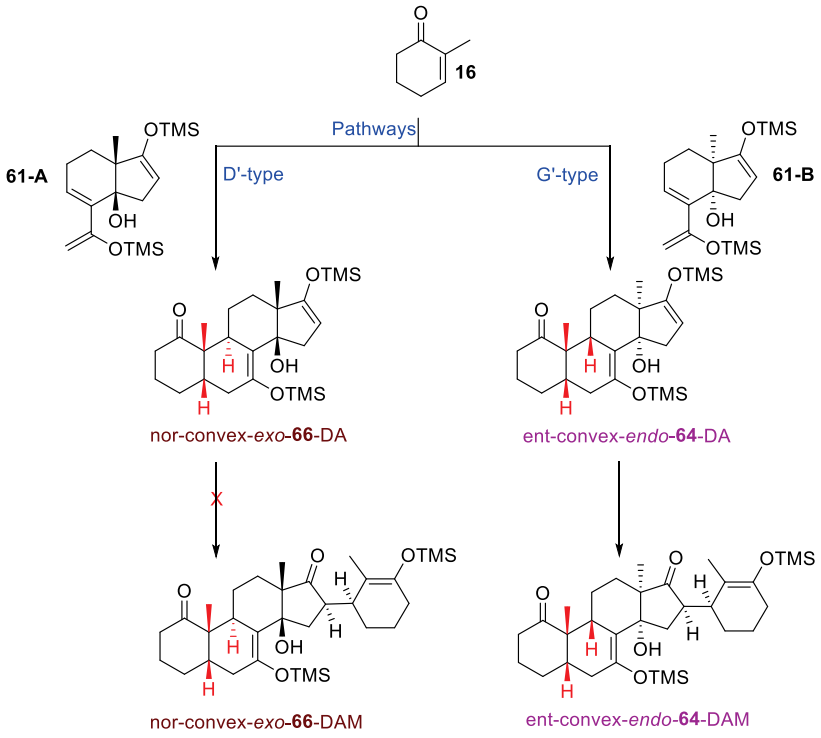

Scheme 20. Possible formation of DAM-adducts **64** and **66**

The reaction coordinates of the Michael addition reaction to afford D'-type Michael adduct (nor-convex-*exo*-**66-DAM**) *via* the transition state D'-type-TS2 and G'-type Michael adduct (ent-convex-*endo*-**64-DAM**) *via* G'-type-TS2 were depicted in **Figure 6**.

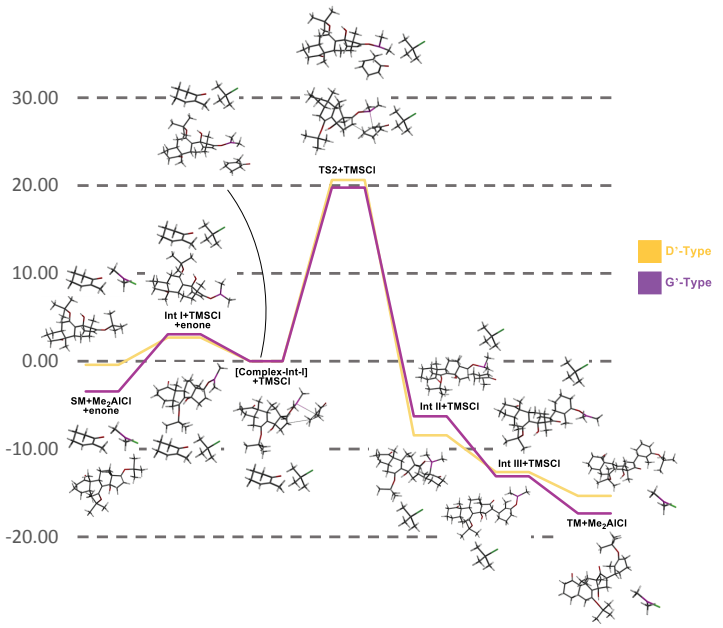

Pathway Type	SM+Me_2AlCl +enone	Int-I+TMSCl +enone	[Complex-Int-I] +TMSCl	TS2+TMSCl	Int-II+TMSCl	Int-III+TMSCl	TM with Me_2AlCl
D` type	−0.41	2.69	0.00	20.63	−8.44	−12.61	−15.33
G` type	−3.44	3.07	0.00	19.76	−6.27	−13.10	−17.33

Figure 6. Reaction coordinates to form DAM-adducts **64** and **66**

The energy differences (TS2 – ([Complex-Int-I]) corresponding to the activation energies for D'-type-TS2 was over ~1 kcal/mol against that for G'-type-TS2. Additionally, the activation energy for the formation of D'-type Michael adduct (nor-convex-*exo*-**66-DAM**) was over 20 kcal/mol, therefore the Michael addition reaction was kinetically prohibited to give the corresponding Michael adduct at low temperature. On the other hand, the activation energy for the formation of G'-type Michael adduct (ent-convex-*endo*-**64-DAM**) was less than 20 kcal/mol. Therefore the Michael addition reaction spontaneously proceeded to afford ent-convex-*endo*-**64-DAM** at low temperature.

In summary, we rationalized the four interesting phenomena (i)–(iv) regarding the parallel kinetic resolution using simplified model substrates (+)-**61-A** and (−)-**61-B**. DFT calculations at B3LYP/6-31G* level showed that some patterns of TSs, such as B-, C-, and H-type-TSs, and E'-type-TS2, were kinetically unfavored structures, and that several stereoisomers, such as D-type DA and G'-type Michael adduct were thermodynamically very stable compounds. Considerations of all the energies of the key intermediates and the transition structures provided reasonable kinetic and thermodynamic behavior of each stereoisomer on the reaction coordinates to uncover the whole aspect of the parallel kinetic resolution during the reaction processes of the Diels–Alder reaction between (*R*)-carvone **35** with (+)-silyl enol ether ((+)-**12-A**) or (−)-silyl enol ether ((−)-**12-B**), followed by the Michael addition reaction.

In conclusion, we have shown that the synthesis of 14β-hydroxysteroids scaffolds was efficiently achieved through highly diastereo/enantioselective Diels–Alder reactions. The synthetic routes which were developed are highly efficient because five steps were sufficient to get the compounds of interest. Finally the presence of the 3-isopropenyl group was potentially highly valuable for the introduction of a 3β-hydroxy group as it has already been shown.[6b] Moreover, DFT studies allowed us to propose reasonable mechanism insights for the DA-reaction being under chemodivergent parallel kinetic resolution control especially the formation of *exo*-DA and *endo*-DAM-adducts. Finally, synthetic approaches to (*ent*)-cardenolides/bufadienolides using our methodology will be described in the near future.

EXPERIMENTAL

General Information. Reactions were carried out under argon with magnetic stirring and degassed solvents. Et_2O and THF were distilled over alumina on a dry solvent station GT S100. Thin layer chromatography (TLC) was carried out on silica gel plates (Merck 60F254) and the spots were visualized under UV lamp (254 or 365 nm) and sprayed with phosphomolybdic acid solution (25 g phosphomolybdic acid, 10 g cerium sulfate, 60 mL H_2SO_4, 940 mL H_2O) followed by heating on a hot

plate. For column chromatography, silica gel (Merck Si 60 40-60 μm) was used. IR spectra were recorded on Bruker Alpha (ATR) spectrophotomer. ^{1}H NMR spectra were recorded at 500 MHz (Bruker AC-500) and ^{13}C NMR spectra at 125 MHz (Bruker AC-500) using the signal of the residual non deuterated solvent as internal reference. Significant ^{1}H NMR data are tabulated in the following order: chemical shift (δ) expressed in ppm, multiplicity (s, singlet; d, doublet; t, triplet; q, quartet; m, multiplet), coupling constants in hertz, number of protons. High-resolution mass spectra (HRMS) were performed on a Agilent 6520 Accurate Mass Q-TOF. High Pressure reactions have been done with a LV 30/16 chamber and a U 101 press coming from the High Pressure Research Control of the Polish Academy of Sciences (Warsaw, Poland).

Experimental procedures, spectroscopic data of all compounds, and Cartesian coordinates of X-ray crystallographic data for (rac)-**17**, (rac)-**18a**, (rac)-**29a**, (+)-**33a**, (+)-**36**, (–)-**36**, (–)-**37a**, and (+)-**51a**, and absolute energies for all calculated structures have been provided in the Supporting Information.

ACKNOWLEDGEMENTS

Support for this work was provided by CNRS, the Université de Strasbourg and ANR Sterob (No. 07-PCVI-0016)). C. P. thanks MRT for financial support. I. S. thanks the Center of Chirality (Tokyo University of Science) for financial support.

REFERENCES AND NOTES

1. (a) Y. J. Shukla, I. A. Khan, P. Geoffroy, and M. Miesch, *Stud. Nat. Prod. Chem.*, 2013, **40**, 327; (b) C. Smith and A. Krygsman, *J. Ethnopharm.*, 2014, **155**, 987.
2. (a) B. Heasley, *Chem. Eur. J.*, 2012, **18**, 3092; (b) H. P. Albrecht, *Cardiac glycosides. In Naturally Occurring Glycosides*, Wiley, New York, 1999, p 83; (c) E. J. Eichhorn and M. Gheorghiade, *Prog. Cardiovasc. Dis.*, 2002, **44**, 251.
3. (a) B. Stenkvist, E. Bengtsson, O. Eriksson, J. Holmquist, B. Nordin, S. Westman-Naeser, and G. E. Eklund, *Lancet*, 1979, **313**, 563; (b) M. Slingerland, C. Cerella, H. J. Guchelaar, M. Diederich, and H. Gelderblom, *Invest. New Drugs*, 2013, **31**, 1087; (c) R. A. Newman, P. Yang, A. D. Pawlus, and K. I. Block, *Mol. Interv.*, 2008, **8**, 36; (d) J. M. Langenhan, J. M. Engle, L. K. Slevin, L. R. Fay, R. W. Lucker, K. R. Smith, and M. Endo, *Bioorg. Med. Chem. Lett.*, 2008, **18**, 670.
4. (a) E. Yoshii, T. Oribe, T. Koizumi, I. Hayashi, and K. Tumura, *Chem. Pharm. Bull.*, 1977, **25**, 2249; (b) G. R. Pettit, L. E. Houghton, J. C. Knight, and F. Bruschweiler, *J. Org. Chem.*, 1970, **35**, 2895; (c) E. Yoshii, T. Oribe, K. Tumura, and T. Koizumi, *J. Org. Chem.*, 1978, **43**, 3946; (d) R. Marini-Bettolo, P. Flecker, T. Y. R. Tsai, and K. Wiesner, *Can. J. Chem.*, 1981, **59**, 1403; (e) K.

Wiesner and T. Y. R. Tsai, *Pure Appl. Chem.*, 1986, **58**, 799; (f) P. Kočovsky and I. Stieborová, *Tetrahedron Lett.*, 1989, **30**, 4295; (g) H. Renata, Q. Zhou, and P. S. Baran, *Science*, 2013, **339**, 59; (h) H. Renata, Q. Zhou, G. Dünstl, J. Felding, R. R. Merchant, C-H. Yeh, and P. S. Baran, *J. Am. Chem. Soc.*, 2015, **137**, 1330.

5. (a) J. F. Lavallée and Deslongchamps, *Tetrahedron Lett.*, 1988, **29**, 6033; (b) R. Ruel and P. Deslongchamps, *Can. J. Chem.*, 1990, **68**, 1917; (c) R. Ruel and P. Deslongchamps, *Can. J. Chem.*, 1992, **70**, 1939; (d) R. Ruel and P. Deslongchamps, *Tetrahedron Lett.*, 1990, **31**, 3961; (e) D. Chapdelaine, J. Belzile, and P. Deslongchamps, *J. Org. Chem.*, 2002, **67**, 5669; (f) Z. Yang, D. Shannon, V. L. Truong, and P. Deslongchamps, *Org. Lett.*, 2002, **4**, 4693; (g) S. Trudeau and P. Deslongchamps, *J. Org. Chem.*, 2004, **69**, 832; (h) H. Zhang, M. S. Reddy, S. Phoenix, and P. Deslongchamps, *Angew. Chem. Int. Ed.*, 2008, **47**, 1272; (i) M. S. Reddy, H. Zhang, S. Phoenix, and P. Deslongchamps, *Chem. Asian J.*, 2009, **4**, 725.
6. (a) M. Honma and M. Nakada, *Tetrahedron. Lett.*, 2007, **48**, 1541; (b) K. Mukai, D. Urabe, S. Kasuya, N. Aoki, and M. Inoue, *Angew. Chem. Int. Ed.*, 2013, **52**, 5300; (c) K. Mukai, S. Kasuya, Y. Nakagawa, D. Urabe, and M. Inoue, *Chem. Sci.*, 2015, **6**, 3383; (d) N. R. Cichowicz, W. Kaplan, Y. Khomutnyk, B. Bhattarai, Z. Sun, and P. Nagorny, *J. Am. Chem. Soc.*, 2015, **137**, 14341; (e) W. Kaplan, H. R. Khatri, and P. Nagorny, *J. Am. Chem. Soc.*, 2016, **138**, 7194; (f) B. Bhattarai and P. Nagorny, *Org. Lett.*, 2018, **20**, 154.
7. (a) L. E. Overman and P. V. Rucker, *Tetrahedron Lett.*, 1998, **39**, 4643; (b) J. Hynes, Jr., L. E. Overman, T. Nasser, and P. V. Rucker, *Tetrahedron Lett.*, 1998, **39**, 4647.
8. (a) M. E. Jung and D. Yoo, *Org. Lett.*, 2011, **13**, 2698; (b) M. E. Jung and M. Guzaev, *J. Org. Chem.*, 2013, **78**, 7518.
9. D. H. Jhuo, B. C. Hong, C. W. Chang, and G. H. Lee, *Org. Lett.*, 2014, **16**, 2724.
10. (a) M. Qian, K. Krishnan, E. Kudova, P. Li, B. D. Manion, A. Taylor, G. Elias, G. Akk, A. S. Evers, C. F. Zorumski, S. Mennerick, and D. F. Covey, *J. Med. Chem.*, 2014, **57**, 171; (b) D. F. Covey, *Steroids*, 2009, **74**, 577; (c) K. Krishnan, B. D. Manion, A. Taylor, J. Bracamontes, J. H. Steinbach, D. E. Reichert, A. S. Evers, C. F. Zorumski, S. Mennerick, and D. F. Covey, *J. Med. Chem.*, 2012, **55**, 1334; (d) D. F. Covey, *Polish J. Chem.*, 2006, **80**, 511; (e) V. Kapras, V. Vyklicky, M. Budesinsky, I. Cisarova, L. Vyklicky, H. Chodounska, and U. Jahn, *Org. Lett.*, 2018, **20**, 946.
11. G. E. Mackay and M. S. Sherburn, *Synthesis*, 2015, **47**, 1.
12. (a) K. Alder and G. Stein, *Angew. Chem.*, 1937, **50**, 510; (b) R. B. Woodward and T. J. Katz, *Tetrahedron*, 1959, **5**, 70; (c) I. Fernández and F. M. Bickelhaupt, *J. Comput. Chem.*, 2014, **35**, 371.

13. (a) B. Ressault, A. Jaunet, P. Geoffroy, S. Goudedranche, and M. Miesch, *Org. Lett.*, 2012, **14**, 366; (b) Y. Wang, A. Jaunet, P. Geoffroy, and M. Miesch, *Org. Lett.*, 2013, **15**, 6198; (c) Preliminary report: C. Peter, B. Ressault, P. Geoffroy, and M. Miesch, *Chem. Eur. J.*, 2016, **22**, 10808.
14. (a) M. Ge, B. M. Stoltz, and E. J. Corey, *Org. Lett.*, 2000, **2**, 1927; (b) B. M. Stoltz, T. Kano, and E. J. Corey, *J. Am. Chem. Soc.*, 2000, **122**, 9044; (c) A. A. Haaksman, B. J. M. Jansen, and A. de Groot, *Tetrahedron*, 1992, **48**, 3121.
15. (a) *endo* adduct **17**: CCDC 957680; (b) The single crystal X-ray diffraction analysis (CCDC 1400288) is related to compound **18a** obtained by TBAF deprotection of *endo*-Michael adduct **18** (see supporting informations): the deprotection reaction was carried out to get crystals suitable for X-ray analysis.
16. M. E. Jung and R. M. Lui, *J. Org. Chem.*, 2010, **75**, 7146.
17. High pressure chemistry: synthetic mechanistic and supercritical applications, ed. by R. van Eldik and F. G. Klärner, Wiley–VCH: Weinheim, 2002.
18. The single crystal X-ray diffraction analysis (CCDC 1405081) is related to compound **29a** obtained by TBAF deprotection of *exo*-adduct **29** (see supporting informations): the deprotection reaction was carried out to get crystals suitable for X-ray analysis.
19. The single crystal X-ray diffraction analysis (CCDC 1571350) is related to compound **33a** obtained by TBAF deprotection of *exo*-adduct **33** (see supporting informations): the deprotection reaction was carried out to get crystals suitable for X-ray analysis.
20. (a) *exo*-adduct (–)-**36**: CCDC 1038730; (b) The single crystal X-ray diffraction analysis (CCDC 1409432) is related to *endo*-Michael-adduct **37a** obtained by TBAF deprotection of *endo*-Michael-adduct **37** (see supporting informations): the deprotection reaction was carried out to get crystals suitable for X-ray analysis; (c) *exo*-adduct (+)-**36**: CCDC 1043760.
21. (a) P. J. Walsh and M. C. Kozlowski, *Fundamentals of Asymetric Catalysis.*, University Science Books, Sausalito, California, 2008, 252; (b) J. R. Dehli and V. Gotor, *Chem. Soc. Rev.*, 2002, **31**, 365.
22. (a) Y. Oikawa, K. Sugano, and O. Yonemitsu, *J. Org. Chem.*, 1978, **43**, 2087; (b) R. Ostwald, P.-Y. Chavant, H. Stadtmüller, and P. Knochel, *J. Org. Chem.*, 1994, **59**, 4143; (c) Compound **39**: J. P. Feng, Z. F. Shi, Y. Li, J. T. Zhang, X. L. Qi, J. Chen, and X. P. Cao, *J. Org. Chem.*, 2008, **73**, 6873; (d) Compound **41**: P. Bolze, G. Dickmeiss, and K. A. Jørgensen, *Org. Lett.*, 2008, **10**, 3753.
23. Z. G. Hajos and D. R. Parrish, *Org. Synth.*, 1985, **63**, 26; (b) S. Bahmanyar and K. N. Houk, *J. Am. Chem. Soc.*, 2001, **123**, 11273; (c) B. Bradshaw and J. Bonjoch, *Synlett*, 2012, **23**, 337; (d) Y. Tang, J. T. Liu, P. Chen, M. C. Lv, Z. Z. Wang, and Y. K. Huang, *J. Org. Chem.*, 2014, **79**, 11729.

24. The single crystal X-ray diffraction analysis (CCDC 1413746) is related to *exo*-adduct (+)**-51a** obtained by TBAF deprotection of *exo*-adduct **51** (see supporting informations): the deprotection reaction was carried out to get crystals suitable for X-ray analysis.
25. All calculations were performed with the program package *Spartan*'10 1.1.0 of Wavefunction, Inc. (https://www.wavefun.com). All structures were optimized and subjected to frequency analysis with the B3LYP/6-31G* method, followed by single-point B3LYP/6-31G* calculations to provide the thermodynamic properties.
26. (a) Titanium enolates formation from silyl enol ethers; T. Mukaiyama, K. Narasaka, and K. Banno, *Chem. Lett*., 1973, **2**, 1011; (b) Boron enolates formation from silyl enol ethers: M. Wada, *Chem. Lett*., 1981, **10**, 153; (c) Boron enolates formation from silyl enol ethers: R. W. Hoffmann, K. Ditrich, and S. Froch, *Liebigs Ann. Chem*., 1987, 977; (d) Boron enolates formation from silyl enol ethers: J. L. Duffy, T. P. Yoon, and D. A. Evans, *Tetrahedron Lett*., 1995, **36**, 9245; (e) Utilities of aluminium enolates: E. A. Jeffery, A. Meisters, and T. Mole, *J. Organomet. Chem*., 1974, **74**, 373; (f) Utilities of aluminium enolates: K. Maruoka, S. Hashimoto, Y. Kitagawa, H. Yamamoto, and H. Nozaki, *J. Am. Chem. Soc*., 1977, **99**, 7705.